Modelling reservoir sediment flushing through a bottom tunnel with an initially covered intake

Sun, Yining; Li, Ji; Cao, Zhixian; Liu, Jinxin; Xu, Huan; Borthwick, Alistair G.L.

Published in:
Applied Mathematical Modelling

DOI:
10.1016/j.apm.2023.10.018

Publication date:
2024

Document version:
Other version

Supporting Information for

Modelling reservoir sediment flushing through a bottom tunnel with an initially covered intake

Yining Sun[a], Ji Li[b], Zhixian Cao[a*], Jinxin Liu[c], Huan Xu[a] and Alistair G.L. Borthwick[d,e]

a State Key Laboratory of Water Resources and Management, Wuhan University, Wuhan 430072, China

b Zienkiewicz Centre for Computational Engineering, Faculty of Science and Engineering, Swansea University, Swansea SA1 8EN, UK

c Changjiang Survey, Planning, Design and Research, Co., Ltd., Wuhan, 430010, China

d Institute for Infrastructure and Environment, University of Edinburgh, Edinburgh EH9 3JL, UK

e School of Engineering, Computing and Mathematics, University of Plymouth, Plymouth PL4 8AA, UK

Correspondence

* Zhixian Cao, State Key Laboratory of Water Resources and Management, Wuhan University, Wuhan 430072, China. E-mail: zxcao@whu.edu.cn

Contents of this file

Text S1

Figures from S2 to S6

Text S1 Mathematical model

S1.1 Reservoir module - a 2D double layer-averaged model

S1.1.1 Model closure

To close the governing equations of the extended 2D double layer-averaged model proposed by Sun et al. (2023), a set of relationships is introduced to determine the water entrainment E_w, sediment exchange fluxes (i.e., entrainment E minus deposition D), interface shear stress, and bed boundary resistance, as per Cao et al. (2015). Following Parker et al. (1986), the water entrainment mass flux E_w is calculated from

$$E_w = e_w \overline{U}_{ws} \tag{S1}$$

where $\overline{U}_{ws} = \sqrt{(U_w - U_s)^2 + (V_w - V_s)^2}$ is the magnitude of the resultant velocity difference between the two layers, (U_w, V_w) are clear-water flow layer-averaged velocity components in the x- and y-directions, (U_s, V_s) are sediment-laden flow layer-averaged velocity components in the x- and y-directions, and the water entrainment coefficient e_w is estimated from

$$e_w = \frac{0.00153}{0.0204 + \mathrm{Ri}} \tag{S2}$$

in which $\mathrm{Ri} = sgc_s h_s / \overline{U}_{ws}^2$ is the Richardson number, and $s = (\rho_s / \rho_w) - 1$ is the specific gravity of sediment, ρ_w is water density, ρ_s is sediment density, g is the acceleration due to gravity, c_s is volumetric sediment concentration, and h_s is the thickness of the lower sediment-laden flow layer. The following formulae are used to calculate the sediment entrainment and deposition fluxes,

$$D = \alpha \omega c_s \left(1 - c_s\right)^m \tag{S3}$$

$$E = \alpha \omega C_e \tag{S4}$$

where α is the saturation recovery coefficient which represents the difference between the near-bed sediment concentration and the depth-averaged sediment concentration. Hindered sediment settling velocity $\omega c_s \left(1 - c_s\right)^m$ is taken into account in Eq. (S3), using the relationship determined by Richardson and Zaki (1997). The power m is estimated from $m = 4.45 R_p^{-0.1}$, in which $R_p = \omega d / \nu$ is the particle Reynolds number, ω is the settling velocity of a single sediment particle in tranquil clear water, calculated using the formula of Zhang and Xie (1993) as

$$\omega = \sqrt{(13.95 \frac{\nu}{d})^2 + 1.09 sgd} - 13.95 \frac{\nu}{d} \tag{S5}$$

in which d is the sediment particle diameter, and ν is the kinematic viscosity of water. In evaluating Eq. (S4), the sediment concentration C_e at capacity is computed as

$$C_e = \frac{q_b}{h_s U_m} \tag{S6}$$

where $U_{ms} = \sqrt{U_s^2 + V_s^2}$ is the resultant velocity of the sediment-laden flow layer, q_b is the transport rate in the capacity regime, determined by Wu (2007):

$$\frac{q_b}{\sqrt{sgd}} = 0.0053 \left[\left(\frac{n'}{n_b} \right) \frac{\tau_{eff}}{\tau_c} - 1 \right]^{2.2} + 0.0000262 \left[\left(\frac{\tau}{\tau_c} - 1 \right) \frac{U_m}{\omega} \right]^{1.74} \tag{S7}$$

where $n' = d^{1/6} / 20$ is the Manning's roughness corresponding solely to grain resistance; n_b is the bed roughness Manning's coefficient; τ is the shear stress at the channel cross-section and estimated as $\rho_c g R J$, where ρ_c is the density of the sediment-laden flow layer, R is the hydraulic radius of the cross-section, and J is the friction slope; τ_{eff} is the effective stress; and

τ_c is the critical shear stress for incipient motion of bed material, approximated by $\tau_c = 0.03(\rho_s - \rho_w)gd$.

A set of relationships is introduced to close the model to determine the shear stresses. Specifically, Manning's equation and the Coulomb friction law are used to determine the combined boundary resistance for the Newtonian fluid and solid phases, according to Li et al. (2018), from

$$\tau_N = \tau_{fb} + \tau_{sb} \tag{S8}$$

where τ_{fb} is the Newtonian fluid stress and τ_{sb} is the solid phase stress. Manning's equation is used to calculate resistance relationships between the upper layer clear water flow, the lower layer sediment-laden flow, and the erodible bed as follows:

$$\tau_{wx} = \rho_w g n_i^2 (U_w - U_s) U_{mw} / h_w^{1/3} \tag{S9a}$$

$$\tau_{wx} = \rho_w g n_i^2 (V_w - V_s) U_{mw} / h_w^{1/3} \tag{S9b}$$

$$\tau_{fbx} = \rho_c g n_b^2 U_s U_{ms} / h_s^{1/3} \tag{S10a}$$

$$\tau_{fby} = \rho_c g n_b^2 V_s U_{ms} / h_s^{1/3} \tag{S10b}$$

where n_i is the Manning's coefficient representing friction at the interface between the sediment-laden flow layer and clear-water flow layer; $U_{mw} = \sqrt{U_w^2 + V_w^2}$ is the resultant velocity of the clear-water flow layer; h_w is the thickness of the clear-water flow layer; and h_s is the thickness of the lower sediment-laden flow layer

The solid resistance in the sediment-laden flow layer is determined by the Coulomb friction law, which expresses the collinearity of shear stress and normal stress through a friction

coefficient $\tan\phi_{bed}$. Following this practice, the solid resistance components are given as follows,

$$\tau_{sbx} = g\cos^2\varphi\left(\rho_s - \rho_w\right)h_s c_s \tan\phi_{bed}\frac{U_s}{\sqrt{U_s^{\,2}+V_s^{\,2}}} \tag{S11a}$$

$$\tau_{sby} = g\cos^2\varphi\left(\rho_s - \rho_w\right)h_s c_s \tan\phi_{bed}\frac{V_s}{\sqrt{U_s^{\,2}+V_s^{\,2}}} \tag{S11b}$$

where $\cos\varphi = 1\Big/\sqrt{1+\left(\partial z_b/\partial x\right)^2+\left(\partial z_b/\partial y\right)^2}$, and φ is the bed angle.

One of the pivotal issues in non-Newtonian fluid simulation is the estimation of the yield stress τ_Y and viscous stress $\tau_V\left(=\mu_Y\gamma\right)$ (in which μ_Y is the fluid consistency and $\gamma=\frac{\partial u}{\partial z}$ is the shear rate), which are determined either by calibration against measured data or by using empirical relations, such as the formulae proposed by Fei et al. (1991):

$$\tau_Y = 0.098\exp\left(8.45\frac{c_s - c_{v0}}{c_{vm}}+1.5\right) \tag{S12a}$$

$$\mu_Y = \mu_0\left(1-k\,c_s/c_{vm}\right)^{-2.5} \tag{S12b}$$

where $c_{vm}=0.92+0.02\log\left(1/d\right)$ is the sediment limiting concentration; $c_{vo}=1.26c_{vm}^{\,3.2}$ is the threshold concentration from Newtonian fluid to non-Newtonian fluid; $k=1+2.0\left(c_s/c_{vm}\right)^{0.3}\left(1-c_s/c_{vm}\right)^4$ is a coefficient; and μ_0 is the dynamic viscosity of water.

Based on the assumption of a linear velocity distribution through the depth, the velocity gradient components of sediment-laden flow at the basal surface are approximated by

$$\left.\frac{\partial u_s}{\partial z}\right|_{z=z_b} = \frac{2U_s}{h_s} \tag{S13a}$$

and

$$\left.\frac{\partial v_s}{\partial z}\right|_{z=z_b} = \frac{2V_s}{h_s}. \tag{S13b}$$

S1.1.2 Geo-failure method

The improved geo-failure method proposed by Hu et al. (2023) is applied in the model. Fig. S1 displays the collapsing process. Firstly, collapsed areas are identified depending on whether the bed slope exceeds the angle of repose $\varphi\left(=30^{\circ}\right)$. In such a case, the collapsed sediments enter the ambient flow, producing a highly concentrated sediment-laden flow layer below the upper clear-water flow layer.

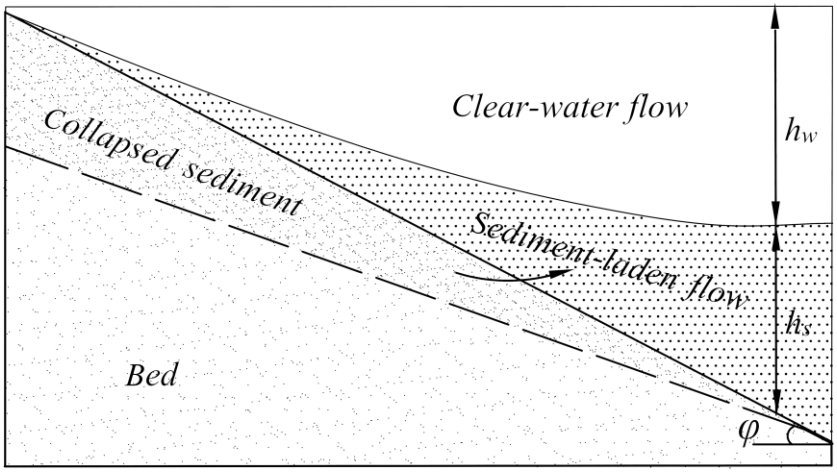

Fig. S1. Process of collapsed sediments entering ambient flow to produce a turbidity current.

The detailed procedure for the geo-failure method is as follows:

(i) Compute bed slopes between cell L with minimum bed elevation and other cells, and identify unstable cells for which the bed slope exceeds the repose angle.

(ii) Modify the bed elevations of unstable cells according to sediment collapse and compute the volume V_m of collapsed sediment. For the collapse process between cell L and the

unstable cell denoted M, the change in bed elevation and volume of collapsed sediment can be described mathematically by

$$\Delta z_b = z_{bm} - z_{bl} - \Delta l_{lm} \tan\varphi \tag{S14}$$

$$V_m = \Delta z_b A_m \left(1 - p\right) \tag{S15}$$

where z_{bl} and z_{bm} are bed elevations at cells L and M; Δz_b is the change in bed elevation at cell M due to sediment collapse; A_m is the area of cell M; and Δl_{lm} is the distance between cells L and M.

(iii) Treat the collapsed sediments as summarized below. Physically, collapsed sediment plays the same role as bed erosion in the momentum conservation relations for sediment-laden flow. The eroded sediments bring zero momentum into the flow (Cao et al., 2017). This is represented by apparent, but not actual, momentum transfer between the sediment-laden flow and bed as shown in the RHS (right-hand side) of Eqs. (S17a and S17b). Besides, the contribution of mass exchange with the bed to mass conservation of the sediment-laden flow is significant in the collapsed area, as characterized by the RHS term in Eqs. (S16, S18 and S19). Notably, whether sediment carried by the flow would become part of the nearby bed entirely depends on the local flow and sediment conditions. If the local sediment is overloaded (i.e., sediment concentration exceeds the transport capacity), then collapsed sediment may become part of the nearby bed through deposition, otherwise, it may be transported away. The resulting mass and momentum equations including the effect of collapsed sediment are:

$$\left(\frac{\partial \eta_s}{\partial t}+\frac{\partial h_s U_s}{\partial x}+\frac{\partial h_s V_s}{\partial y}\right)_{sub}=\left(E_w+\frac{E_c}{1-p}\right)_{sub} \tag{S16}$$

$$\begin{aligned}\left(\frac{\partial h_s U_s}{\partial t}+\frac{\partial}{\partial x}\left[h_s U_s^2+0.5g\left(\eta_s^2-2\eta_s z_b\right)\right]+\frac{\partial}{\partial y}\left(h_s U_s V_s\right)\right)_{sub}&=\left(-g\eta_s\frac{\partial z_b}{\partial x}-\frac{\rho_w g}{\rho_c}h_s\frac{\partial h_w}{\partial x}\right.\\ -\frac{\left(\rho_0-\rho_c\right)U_s}{\left(1-p\right)\rho_c}\left(E-D+E_c\right)+\frac{\left(\rho_s-\rho_w\right)c_s U_s E_w}{\rho_c}+\frac{\rho_w E_w U_w}{\rho_c}-\frac{\left(\rho_s-\rho_w\right)g h_s^2}{2\rho_c}\frac{\partial c_s}{\partial x}&\\ \left.+\frac{\tau_{wx}}{\rho_c}-\frac{\tau_{Nx}}{\rho_c}-\frac{1}{\rho_c}\left[\left(\frac{\tau_Y}{|\gamma_x|}+\mu_Y\right)\gamma_x\right]\right|_{z=z_b}\Bigg)_{sub}&\end{aligned} \tag{S17a}$$

$$\begin{aligned}\left(\frac{\partial h_s V_s}{\partial t}+\frac{\partial}{\partial x}\left(h_s U_s V_s\right)+\frac{\partial}{\partial y}\left[h_s V_s^2+0.5g\left(\eta_s^2-2\eta_s z_b\right)\right]\right)_{sub}&=\left(-g\eta_s\frac{\partial z_b}{\partial y}-\frac{\rho_w g}{\rho_c}h_s\frac{\partial h_w}{\partial y}\right.\\ -\frac{\left(\rho_0-\rho_c\right)V_s}{\left(1-p\right)\rho_c}\left(E-D+E_c\right)+\frac{\left(\rho_s-\rho_w\right)c_s V_s E_w}{\rho_c}+\frac{\rho_w E_w V_w}{\rho_c}-\frac{\left(\rho_s-\rho_w\right)g h_s^2}{2\rho_c}\frac{\partial c_s}{\partial y}&\\ \left.+\frac{\tau_{wy}}{\rho_c}-\frac{\tau_{Ny}}{\rho_c}-\frac{1}{\rho_c}\left[\left(\frac{\tau_Y}{|\gamma_y|}+\mu_Y\right)\gamma_y\right]\right|_{z=z_b}\Bigg)_{sub}&\end{aligned} \tag{S17b}$$

$$\left(\frac{\partial h_s c_s}{\partial t}+\frac{\partial h_s U_s c_s}{\partial x}+\frac{\partial h_s V_s c_s}{\partial y}\right)_{sub}=\left(E-D+E_c\right)_{sub} \tag{S18}$$

$$\left(\frac{\partial z_b}{\partial t}\right)_{sub}=\left(\frac{D-E-E_c}{1-p}\right)_{sub} \tag{S19}$$

where the subscript 'sub' refers to specific cells that receive collapsed sediment; $E_c=\frac{V_m}{A_m\Delta t}$ is the rate of collapse per unit width; and Δt is the time step, which is controlled by the Courant-Friedrichs-Lewy condition.

S1.2 Water and sediment exchange between the reservoir and bottom tunnel

Flows at the bottom outlet in reservoirs are typically supercritical and pressurized. For such problems, the method of characteristics usually yields unsatisfying results for lack of shock-capturing ability. For the source terms, the spatial differential terms are calculated with the

first-order backward difference scheme and the first-order forward difference scheme in the reservoir module and bottom tunnel module, respectively, which avoids the influence of boundary conditions on the source term calculation. For the calculation of water and sediment exchange fluxes at the inner boundary, the present study adopts the following procedure:

A ghost cell is set at the upstream boundary of the bottom tunnel module. Physical variables (i.e., sediment concentration, flow discharge, and piezometric head) of the ghost cell are determined based on variables of several 2D cells near the tunnel intake. Specifically, at the inner boundary, i.e., the tunnel intake, the approach velocity head is neglected (Xu et al., 2023), and hence the flow pressure p_r is assumed hydrostatic,

$$p_r = \begin{cases} \rho_w g h' & 0 < h' < h_w \\ \rho_w g h_w + \rho_c g \left(h' - h_w \right) & h_w < h' < \eta_s - z_b \end{cases} \tag{S24}$$

where h' is the depth from the free water surface. The flow pressure difference between the upper and bottom edges of the tunnel intake, which can be converted to the piezometric head p_r'. Besides, the discharge Q_v of the ghost cell is the summation of the discharge of 2D cells near the tunnel intake, and the volumetric sediment concentration c_v of the ghost cell is relative to the volumetric sediment concentration c_{sj} of 2D cells near the tunnel intake. The calculation of those variables mainly depends on the position of the interface η_s relative to the floor and roof level of the tunnel intake, such that

(i) if the interface elevation η_s is higher than the roof of the tunnel intake,

$$p_r' = \begin{cases} 0 & \overline{z_{br}} > z_{bh} \\ 0.5\rho_c g\left(h_t - \overline{z_{br}}\right)\left(2\overline{h_s} - h_t + \overline{z_{br}}\right) + \rho_w g\,\overline{h_w}\left(h_t - \overline{z_{br}}\right) & z_{bt} < \overline{z_{br}} \le z_{bh} \\ 0.5\rho_c g\left(h_t - z_{bt}\right)\left(2\overline{h_s} + 2\overline{z_{br}} - h_t - z_{bt}\right) + \rho_w g\,\overline{h_w}\left(h_t - z_{bt}\right) & \overline{z_{br}} \le z_{bt} \end{cases} \quad \text{(S25a)}$$

$$Q_v = \sum_{j=1}^{N_j}\left(h_{sj}U_{sj}\Delta y\right) \quad \text{(S25b)}$$

$$c_v = \sum_{j=1}^{N_j} c_{sj}/N_j \quad \text{(S25c)}$$

(ii) if the interface elevation η_s is located between the floor and roof of the tunnel intake,

$$p_r' = \begin{cases} \rho_w g h_w\left(h_t - \overline{z_{br}}\right) - 0.5\rho_w g\left(\overline{h_s} - h_t + \overline{z_{br}}\right)^2 + 0.5\rho_c g\,\overline{h_s}^2 & z_{bt} < \overline{z_{br}} \le z_{bh} \\ \rho_w g h_w\left(h_t - z_{bt}\right) - 0.5\rho_w g\left(\overline{h_s} - h_t + \overline{z_{br}}\right)^2 + 0.5\rho_c g\left(z_{bt} - \overline{h_s} - \overline{z_{br}}\right)^2 & \overline{z_{br}} \le z_{bt} \end{cases} \quad \text{(S26a)}$$

$$Q_v = \sum_{j=1}^{N_j}\left(h_{sj}U_{sj}\Delta y + h_{wj}U_{wj}\Delta y\right) \quad \text{(S26b)}$$

$$c_v = \sum_{j=1}^{N_j}\left[\left(\eta_{sj} - z_{bt}\right)c_{sj}/h_t\right]/N_j \quad \text{(S26c)}$$

(iii) if the interface elevation η_s is lower than the floor of the tunnel intake,

$$p_r' = 0.5\rho_w g\left(h_t - z_{bt}\right)\left(2(\overline{h_w} + \overline{h_s} + \overline{z_{br}}) - h_t - z_{bt}\right) \quad \text{(S27a)}$$

$$Q_v = \sum_{j=1}^{N_j}\left(h_{wj}U_{wj}\Delta y\right) \quad \text{(S27b)}$$

$$c_v = 0 \quad \text{(S27c)}$$

where N_j is the transverse cell number at the inner boundary near the tunnel intake in the reservoir module; Q_v is the discharge of the ghost cell; c_v is the sediment concentration of the ghost cell; $\overline{z_{br}} = \left(\sum z_{bj}\right) / N_j$ is the mean bed elevation at cells near the tunnel intake in the reservoir module; $\overline{h_s} = \left(\sum h_{sj}\right) / N_j$ is the mean thickness h_{sj} of the sediment-laden flow; $\overline{h_w} = \left(\sum h_{wj}\right) / N_j$ is the mean depth h_{wj} of clear-water flow; z_{bt} is the bottom bed elevation of the tunnel intake; z_{bh} is the roof elevation of the tunnel intake; $h_t = z_{bh} - z_{bt}$ is the difference between the roof elevation and bottom bed elevation of the intake.

Then, the water and sediment exchange flux at the upstream boundary of the 1D bottom tunnel module can be computed by the HLLC Riemann solver (Toro, 2001; Liu et al., 2022), and the summation of the fluxes at the downstream boundary of the 2D reservoir module near the tunnel intake must equal the foregoing result. Thus, three kinds of conditions should be considered: (A) if the interface elevation η_s between the clear-water and sediment-laden flow layers is above the roof level of the tunnel intake, only sediment-laden flow at high concentration enters the tunnel, and the flux from the reservoir module to the bottom tunnel module depends solely on the sediment-laden flow layer; (B) if the interface elevation η_s is below the roof level of the tunnel intake, flows from both the sediment-laden flow layer and clear-water flow layer enter the tunnel, and the flux calculation depends on quantities from both layers, following mass and momentum conservation laws; (C) if the interface elevation η_s is below the floor level of the tunnel intake, clear water enters the tunnel, and the flux calculation solely depends on quantities from the clear-water flow layer.

Specifically, under the above conditions, for 2D cells with double flow layers at the downstream boundary near the tunnel intake in the reservoir module, the convection terms of the

exchanged fluxes of different layers are allocated according to the proportion of each layered flow discharge to the total flow discharge. Besides, under conditions A and C, the pressure terms of the exchanged fluxes are evenly distributed to the corresponding flow layer of each 2D cell with a single flow layer. Under condition B, such parts of exchanged fluxes are firstly distributed to each 2D cell with double flow layers on average, and then, they are redistributed according to the proportion of the pressure difference between the interface of two layers and the floor or roof of the tunnel intake, respectively. Through this procedure, the 2D reservoir module is integrated with the 1D bottom tunnel module with mass and momentum conservation strictly preserved.

Figures from S2 to S6

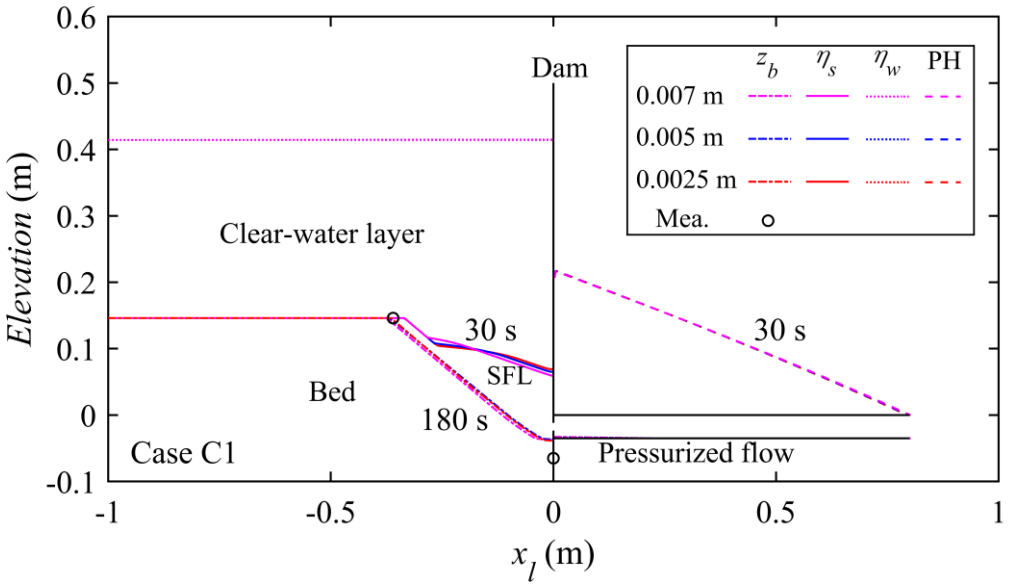

Fig. S2. Case C1 - Computed profiles (η_s : interface elevation, PH: piezometric head, and z_b : bed elevation) along the central axis using three different space steps ($0.007\,\text{m}, 0.005\,\text{m}, 0.0025\,\text{m}$). Measured bed profiles are shown.

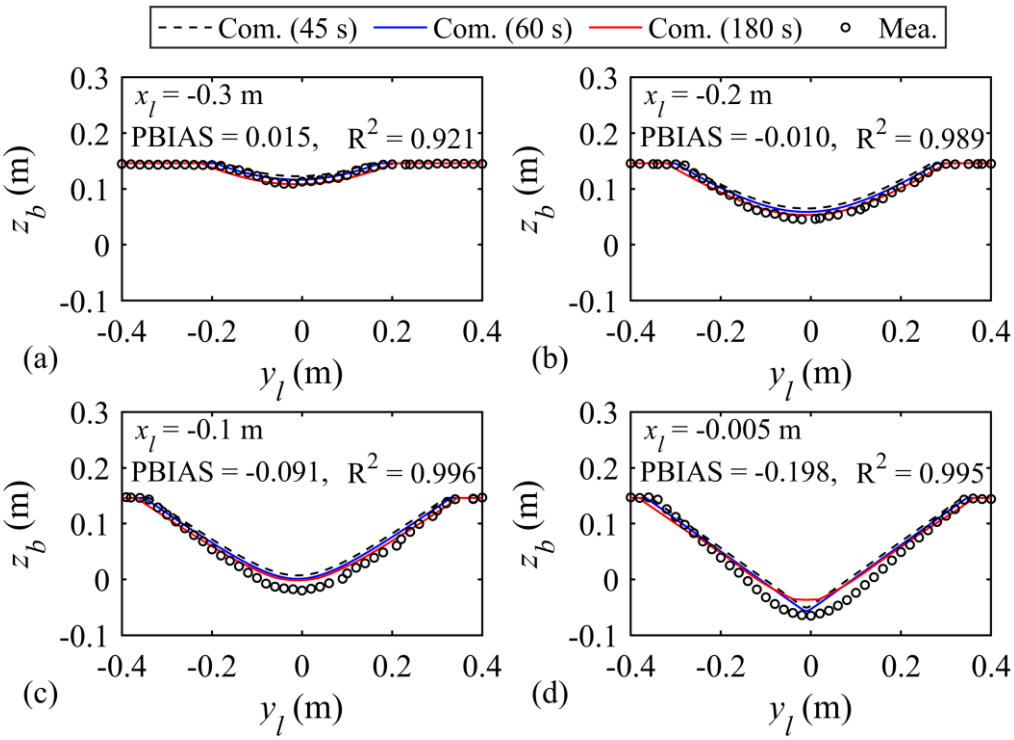

Fig. S3. Case C1 - Computed and measured (Xu et al., 2023) cross-sectional profiles of bed elevation: (a) $x_l = -0.3\,\text{m}$; (b) $x_l = -0.2\,\text{m}$; (c) $x_l = -0.1\,\text{m}$; (d) $x_l = -0.005\,\text{m}$.

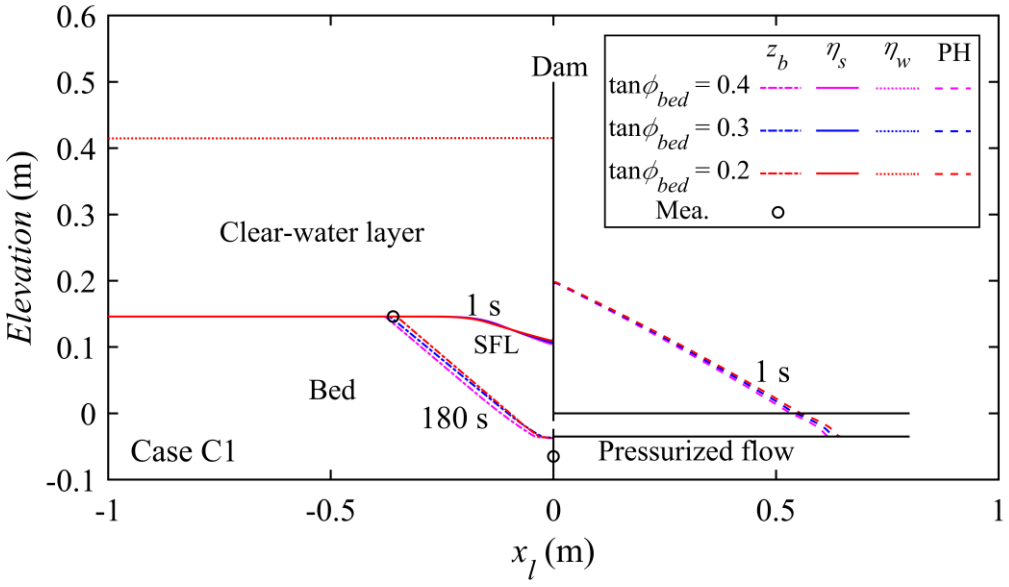

Fig. S4. Case C1 - Computed profiles (η_s : interface elevation, PH: piezometric head, and z_b : bed elevation) along the central axis using three different friction coefficient values ($\tan\phi_{bed} = 0.4, 0.3, 0.2$). Measured bed profiles are shown.

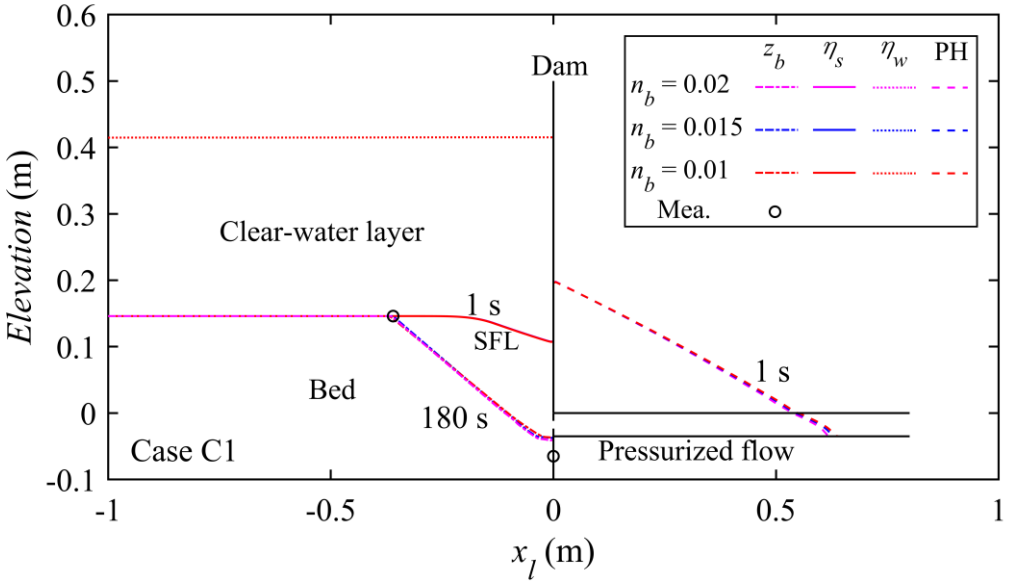

Fig. S5. Case C1 - Computed profiles (η_s : interface elevation, PH: piezometric head, and z_b : bed elevation) along the central axis using three different Manning's roughness coefficients ($n_b = 0.02, 0.015, 0.01 \mathrm{m}^{-1/3}\mathrm{s}$). Measured bed profiles are shown.

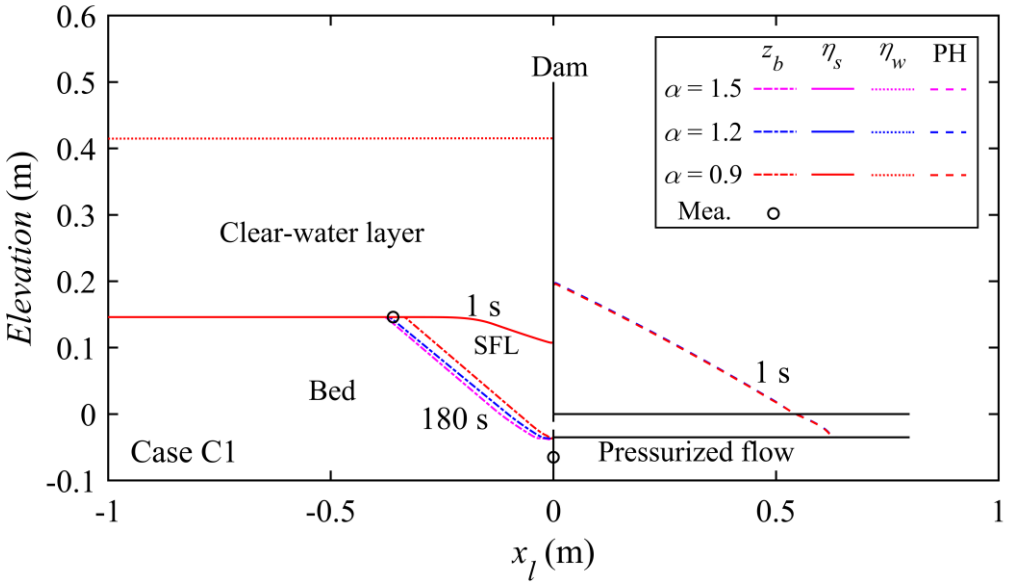

Fig. S6. Case C1 - Computed profiles (η_s : interface elevation, PH: piezometric head, and z_b : bed elevation) along the central axis using three different saturation recovery coefficients ($\alpha = 1.5, 1.2, 0.9$). Measured bed profiles are shown.